International Journal of Biological Macromolecules 52 (2013) 358–367

Contents lists available at SciVerse ScienceDirect

International Journal of Biological Macromolecules

journal homepage: www.elsevier.com/locate/ijbiomac

Dynamics of laser-excited stacked adenines: Semiclassical simulations

Yusheng Dou[a,b,*], Zhicheng Liu[a], Shuai Yuan[a], Wenying Zhang[a], Hong Tang[a], Jiashe Zhao[c], Weihai Fang[d], Glenn V. Lo[b]

[a] Institute of High Performance Computing and Applications, Chongqing University of Posts and Telecommunications, Chongqing 400065, China
[b] Department of Physical Sciences, Nicholls State University, P.O. Box 2022, Thibodaux, LA 70310, USA
[c] Key Laboratory of Synthetic and Natural Functional Molecule Chemistry of Ministry of Education, Shaanxi Key Laboratory of Physics Inorganic Chemistry, Department of Chemistry, Northwest University, Xi'an 710069, China
[d] Department of Chemistry, Beijing Normal University, Beijing 100875, China

ARTICLE INFO

Article history:
Received 24 July 2012
Received in revised form 1 October 2012
Accepted 6 October 2012
Available online 17 October 2012

Keywords:
π-Stacked
Adenine
Bonded excimer
Semiclassical dynamics simulation

ABSTRACT

The nonradiative decay of a π-stacked pair of adenine molecules, following laser excitation, was studied by semiclassical dynamics simulations. Two deactivation pathways were characterized. One pathway involves an ultrafast internal conversion within ~600 fs induced by an out-of-plane vibration of the H atom and deformation of the pyrimidine ring at the C_2 site. A slower process (~2400 fs) involves covalent bond formation between the stacked molecules, which lowers the excimer state energy and inhibits the deformation of the pyrimidine ring; the decay is also induced by an out-of-plane vibration of the H atom at the C_2 site of the pyrimidine ring.

1. Introduction

Exposure of DNA to UV radiation in 200–300 nm range results in strong electronic excitations, which could lead to the photochemical reactions causing DNA damage [1–3]. Therefore, a rapid and efficient release of the excess electronic energy by excited DNA is essential to life. This characteristic of DNA molecules has attracted research interest for least a couple of decades [4–12]. In recent years, femtosecond laser spectroscopy combined with high level quantum mechanical calculations has provided many insights into the mechanisms responsible for the quick dissipation of the excess electronic energy. It is firmly established that highly efficient nonradiative decay pathways exist in DNA molecules, assuring that most excited molecules quickly relax to the electronic ground state without leading to harmful reactions.

The mechanisms for the fast nonradiative decay of monomer DNA bases are fairly well established. The vast majority of electronically excited nucleobases decay to the ground state on a subpicsecond timescale through conical intersections (CI) between the lowest electronic excited-state and the ground state. The conical intersections are accessed, in most cases, via out-of-plane deformations of the pyrimidine ring [2]. The excited-state dynamics of DNA and nucleobase multimers show different nonradiative decay pathways because of interbase interactions, including base stacking and base pairing, and base-solvent interactions [13–16]. Single-stranded polyadenine oligomers [$(dA)_n$], in which base paring is absent, show an ultrafast and a slower nonradiative decay channels [14,17–19]. It has been proposed that the fast decay channel, or monomer-like decay pathway, comes from poorly stacked bases while the slow decay channel is due to interbase stacking interaction.

To understand the nature of electronic excitations, different hypotheses have been proposed. One sophisticated model proposed by Kohler and co-workers [14,20] is that stacked bases are initially excited to an exciton state, which is formed by dipolar coupling of excited states of base monomers. The exciton state decays in less than 1 ps to an excimer/exciplex state that involves just two bases. The decay from the excimer/exciplex state to the ground state usually occurs at a longer time scale. This model is now generally accepted.

The formation of a delocalized excimer state slows down ultrafast nonradiative decay [21,22]. The ab initio calculations at CASPT2 level [23] for two stacked adenines of different arrangements favor a mechanism involving two possible decay pathways. In this mechanism, unstacked or poorly stacked pairs of bases relax to the ground state by an ultrafast internal conversion through the conical intersection between the lowest excited state and ground state of the monomer. On the other hand, an excimer state formed between intrastrand stacked bases exhibits a slower decay time to the ground state because of an energy barrier along the path

* Corresponding author at: Department of Physical Sciences, Nicholls State University, P.O. Box 2022, Thibodaux, LA 70310, USA. Tel.: +1 985 448 4880; fax: +1 985 448 4927.
E-mail address: Yusheng.Dou@nicholls.edu (Y. Dou).

0141-8130/$ – see front matter © 2012 Elsevier B.V. All rights reserved.
http://dx.doi.org/10.1016/j.ijbiomac.2012.10.006

toward the conical intersection of the monomer [23]. It has been suggested [24] that the excimer state has a charge-transfer character and the state lifetime is correlated with the energy required to transfer an electron from one base to its stacked neighbor. An alternative explanation for the slow decay channel is that the base stacking hinders the out-of-plane deformations of the pyrimidine ring [25].

The aforementioned calculations are useful for understanding the main features of the mechanisms behind the ultrafast nonradiative decay dynamics of excited-state of stacked adenines. However, these calculations are incapable of describing the time-dependent properties of the deactivation process. QM/MM calculations are performed along one or two reaction coordinates with other coordinates fixed and, consequently, are inadequate for characterizing a real deactivation process where all reaction coordinates are significantly involved.

In this work, we study the dynamics of nonradiative decay of two stacked adenines following excitation by an ultrafast laser pulse using a semiclassical dynamics simulation technique. In our simulations, all the degrees of freedom of the system are included in the calculations and the laser pulse is explicitly coupled to electrons. By monitoring the nuclear motions triggered by a specific laser pulse, we are able to describe a realistic nonradiative decay pathway. Examining the interplay of the electronic and nuclear motions allows us to study the influence of different vibrational modes on the nonradiative decay process of stacked adenines. The results provide complementary information for understanding the nonradiative decay process of stacked adenines.

2. Methodology

Our technique for this study is semiclassical electron-radiation-ion dynamics (SERID). A detailed description of this method has been published elsewhere [26,27] and only a brief description is presented here. In this method, the valence electrons are treated with a quantum mechanical approach while both the radiation field and the motion of the nuclei are treated classically. The one-electron states are updated by solving the time-dependent Schrödinger equation at each time step (usually 0.05 femtosecond in duration) in a nonorthogonal basis,

$$i\hbar\frac{\partial\boldsymbol{\Psi}_j}{\partial t} = S^{-1}\cdot\mathbf{H}\cdot\boldsymbol{\Psi}_j \tag{1}$$

where **S** represents the overlap matrix of the molecular orbitals. The vector potential **A** of the radiation field is included in the electronic Hamiltonian via the time-dependent Peierls substitution [28]

$$H_{\mathrm{ab}}\left(\mathbf{X}-\mathbf{X}'\right) = H^0_{\mathrm{ab}}\left(\mathbf{X}-\mathbf{X}'\right)\exp\left(\mathbf{A}\cdot\left(\mathbf{X}-\mathbf{X}'\right)\right) \tag{2}$$

where $H_{\mathrm{ab}}(X-X')$ is the Hamiltonian matrix element for basis functions a and b on atoms at position of **X** and **X**′ respectively, and $q=-e$ is the charge of the electron.

The forces acting on nucleus or ions are computed by the Ehrenfest equation using an "on the fly" model:

$$M_l\frac{d^2X_{l\alpha}}{dt^2} = -\frac{1}{2}\sum_j\boldsymbol{\Psi}_j^+\cdot\left(\frac{\partial\mathbf{H}}{\partial X_{l\alpha}} - i\hbar\frac{1}{2}\frac{\partial\mathbf{S}}{\partial X_{l\alpha}}\cdot\frac{\partial}{\partial t}\right)\cdot\boldsymbol{\Psi}_j - \partial U_{\mathrm{rep}}/\partial X_{l\alpha} \tag{3}$$

where U_{rep} is the effective nuclear–nuclear repulsive potential and $X_{l\alpha}=\left\langle\hat{X}_{l\alpha}\right\rangle$ is the expectation value of the time-dependent Heisenberg operator for the α coordinate of the nucleus labeled by l (with $\alpha=x,y,z$).

The Hamiltonian matrix **H**, overlap matrix **S**, and effective nuclear-nuclear repulsive potential U_{rep} are calculated in the density-functional tight-binding approximation (DFTB) [29,30]. These quantities are functions only of the nuclear distance and the results from the calculations for a dimer can be tabulated and employed in the time-dependent calculations. The basis functions used in the present simulations are the 1s atomic orbital of H and the valence s and p orbitals of C and N. No distinctions are made for spin-up and spin-down states. In this approach, the electronic energy of a molecule can be written as

$$E_{\mathrm{elec}} = \sum_{i=\mathrm{occ}} n_i\varepsilon_i + \sum_{\alpha>\beta}U_{\mathrm{rep}}(|X_\alpha - X_\beta|) \tag{4}$$

where ε_i and n_i are the eigenvalue and occupation number of Kohn–Sham orbital ***i***. The first summation goes over all occupied orbitals. Potential energy $U_{\mathrm{rep}}(|X_\alpha - X_\beta|)$ is a function of the inter-atom distance.

The DFTB method has been successfully applied to study the ground state properties of various systems, including solid state physics and biochemical problems [31,32]. More recently, DFTB has been used for a simplified calculation for the DFDFT response equation [33]. The calculation was found to be reliable in reproducing excited state energies and geometries of ab initio TDDFT with remarkable quality. Applied to an amino acid model system, DFTB was found to be a promising method to describe polarization and charge-transfer effects in large systems [34], like the system that we investigate in this paper. We have previously applied the SERID technique to study the photoisomerization mechanism of azobenzene by $n\pi^*$ excitation [35] and isomerization quantum yields [36] for $n\pi^*$ and $\pi\pi^*$ excitations. The method has also been used in biologically-relevant studies (nonadiabatic decay for adenine [5], photodissociation of cyclobutane thymine dimer [37], and photoinduced dimerization of thymine [38]) and the results were found to be consistent with experimental observations. A limitation of this method is that the simulation trajectory moves along a path produced by averaging over all the terms in the Born–Oppenheimer expansion [39–43],

$$\boldsymbol{\Psi}^{\mathrm{total}}(X_n,x_e,t) = \sum_i\boldsymbol{\Psi}_i^n(X_n,t)\,\boldsymbol{\Psi}_i^e(x_e,X_n) \tag{5}$$

rather than following the time evolution of a single potential energy surface – which is approximately decoupled from all the others [44–46]. (Here, X_n and X_n represent the sets of nuclear and electronic coordinates respectively, and the Ψ_i^e are eigenstates of the electronic Hamiltonian at fixed X_n.) The strengths of the present approach include (1) the inclusion of all $3N$ nuclear degrees of freedom, and (2) the incorporation of both the excitation due to a laser pulse and the subsequent de-excitation at an avoided crossing near a conical intersection.

Fig. 1 shows the structure and atomic numbering scheme for an adenine molecule. To produce a ground state equilibrium geometry for these simulations, a "B configuration" consisting of two adjacent adenines is taken at random from a B-type duplex DNA strand, $(dA)_{20}$; the ribose and phosphate groups are ignored. The equilibrated geometry, obtained after the running the simulation through 1000 fs, is shown in Fig. 2. We will refer to the adenine molecule that ends up being excited as A and its atoms are labeled as N_1, C_2, etc.; corresponding atoms in the other molecule, referred to as A', are labeled as N'_1, C'_2, etc. The two molecules are stacked such that the interatomic distances (C_4—C'_4) and (C_5—C'_5) are 4.01 and 3.81 Å, respectively, and the dihedral angle (C_4—C_5—C'_5—C'_4) is 36.2°. An alternate view ("from the top") of the stacked adenines is shown on the right side of Fig. 2. Starting with the equilibrated geometry in Fig. 2, the simulation was run for an additional 100 fs; the geometries obtained at 1-fs intervals were used as initial geometries subjected to laser excitation. A laser pulse with a Gaussian profile (25 fs fwhm and 3.90 eV photon energy) was applied. This energy was selected to match the energy gap between the HOMO and LUMO. This energy is lower than the vertical excitation energy

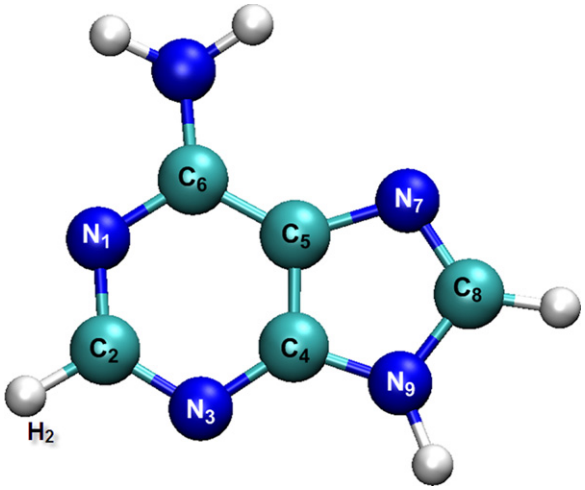

Fig. 1. Structure and atomic labeling for the adenine molecules.

of 5.04 eV for two stacked adenines with a very similar geometry calculated at the ab initio CASPT2 level [23] because of the inherent limitation of DFT approximation.

It should be mentioned here that, in order to describe the interaction energy of **π–π** stacked nucleobases, an empirical dispersion energy correction was used in the calculation. The results of the calculations demonstrated reasonably good agreement between the current method and other empirical methods, such as MP2, for the energy of hydrogen bonding and stacking interactions for a wide range of nucleic acid base pairs [47].

3. Results

For each initial geometry, the fate of the excited system was found to be essentially the same as long the laser fluence is sufficient to cause electronic excitation of one of the adenine molecules but not bond breaking. Of the 100 trajectories, one representative for each initial geometry, 62 show a noticeable interaction between the stacked adenines and a well-defined decay process. The other (38) trajectories lead to a simple separation of the two adenine molecules and will not be discussed. Of the 62 trajectories, 6 were found to undergo a fast nonradiative deactivation; 37 were found to undergo a slow deactivation process that involve formation of a covalent bond between the stacked adenines and the rest show behavior similar to that discussed in an earlier publication [48] (where an "B-like configuration" was selected as initial geometry). Two trajectories, representative of the 6 and 37 aforementioned trajectories, are discussed below.

3.1. Fast nonradiative deactivation process

Six trajectories were found to undergo a fast nonradiative decativation. The analysis of a representative trajectory is summarized in Figs. 3–8. Six snapshots from the simulation are shown in Fig. 3. Starting with the geometry adapted from the ground state B-form DNA (Fig. 3a), the bottom molecule is electronically excited by the laser pulse (fluence = 31.68 J/m^2). The excited molecule undergoes an out-of-plane vibration of the H_2 atom and the deformation of the pyrimidine ring at the C_2 site from 240 fs to 570 fs (Fig. 3b–e), while the unexcited molecule remains stable for this period of time. Two stacked molecules move away from each other at 720 fs (Fig. 3f).

Fig. 4a–c present the time profiles for the C_4—N_3—C_2—H_2, N_1—C_2—N_3—C_4, and C_8—N_7—C_5—C_6 dihedral angles, respectively. The changes in the dihedral angles correspond to the out-of-plane vibration of the H_2 atom, the deformation of the pyrimidine ring at the C_2 site, and the relative position of the pyrimidine and imidazole rings. For comparison, the same dihedral angles are also presented for the unexcited molecule in Fig. 4a–c. Fig. 4 shows that the amplitude of the out-of-plane vibration of the H_2 atom of the excited molecule reaches a maximum at ~580 fs where the dihedral angle becomes less than 60° (its initial value is 180°); the deformation at the C_2 site of the excited molecule also reaches a maximum at 580 fs. The C_8—N_7—C_5—C_6 angle reaches a minimum of about 140° just before 600 fs; the initial value, before laser excitation is 180°. On the other hand, the corresponding dihedral angles of the unexcited molecule remain about the same during the simulation.

The variations with time of the HOMO−1, HOMO, LUMO, and LUMO+1 energies of two stacked molecules are presented in Fig. 5, and the time-dependent population of these frontier molecular orbitals is shown in Fig. 6. Fig. 5 shows that there is an avoided crossing between the HOMO and LUMO with the energy gap being 0.04 eV at 580 fs. Fig. 6 shows electronic excitation being achieved at the end of the laser pulse (~50 fs); about 1.5 electrons are transferred from the HOMO to the LUMO. The HOMO is a π orbital and the LUMO is π^* orbital. This excitation promotes the adenine molecule from the electronic ground state to a low-lying state $\pi\pi^*$ [5]. The coupling between the HOMO and LUMO at about 580 fs leads to a transfer of electrons from the LUMO to the HOMO. This eventually brings the stacked adenine molecules from the low-lying $\pi\pi^*$ state to the electronic ground state. Shortly after the avoided crossing, both the LUMO and HOMO levels move toward their initial values.

Variations with time of three bond lengths, C_2—N_3 and N_3—C_4, and C_4—C_5, of the excited molecule are plotted in Fig. 7. Variations of the same bond lengths for the unexcited molecule are also shown. The C_2—N_3 bond stretches from an initial value of 1.33 Å to about 1.47 Å after 100 fs until ~600 fs, when it shortens to about its initial length; the bond length remains more or less the same for the rest of the simulation time. The C_4—C_5 bond shows similar variations as

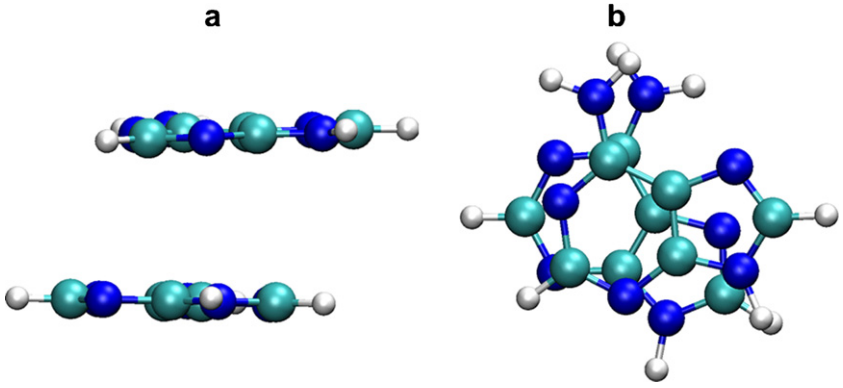

Fig. 2. Stacked adenines: (a) top-view, (b) side-view.

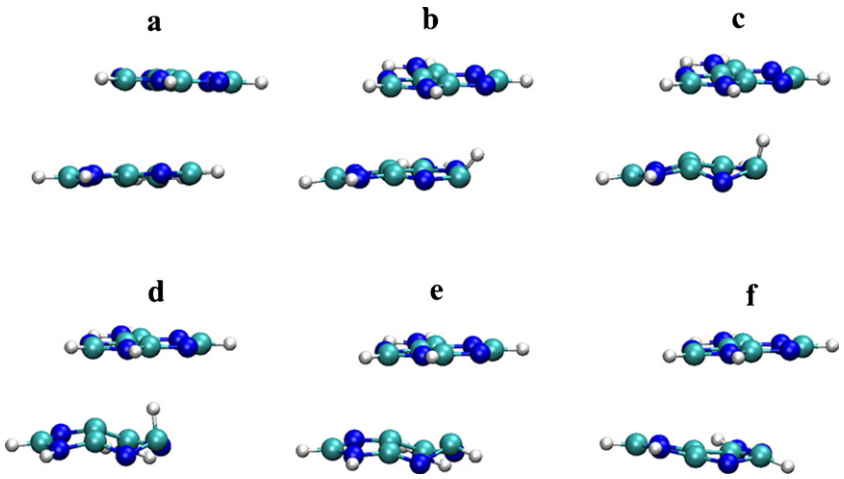

Fig. 3. Snapshots taken from the simulation of two stacked adenine molecules at (a) 0, (b) 240, (c) 340, (d) 570, (e) 610, and (f) 720 fs. The molecule at the bottom is subjected to the irradiation of a 25 fs (fwhm) laser pulse with a fluence of 31.68 J/m^2 and photon energy of 3.9 eV.

the C_2—N_3 bond. On the other hand, the N_3—C_4 bond shrinks from a beginning value of 1.42 Å to 1.33 Å after 100 fs, then expands to about 1.40 Å in length at ~600 fs and beyond.

The simulation results presented above show that the laser pulse promotes one molecule (*A*) from the electronic ground state to the low-lying state $\pi\pi^*$ by the excitation of electrons from the HOMO to LUMO. This is consistent with the changes in the C_2—N_3, N_3—C_4, and C_4—C_5 bond lengths (Fig. 7). At the $\pi\pi^*$ state the molecule no

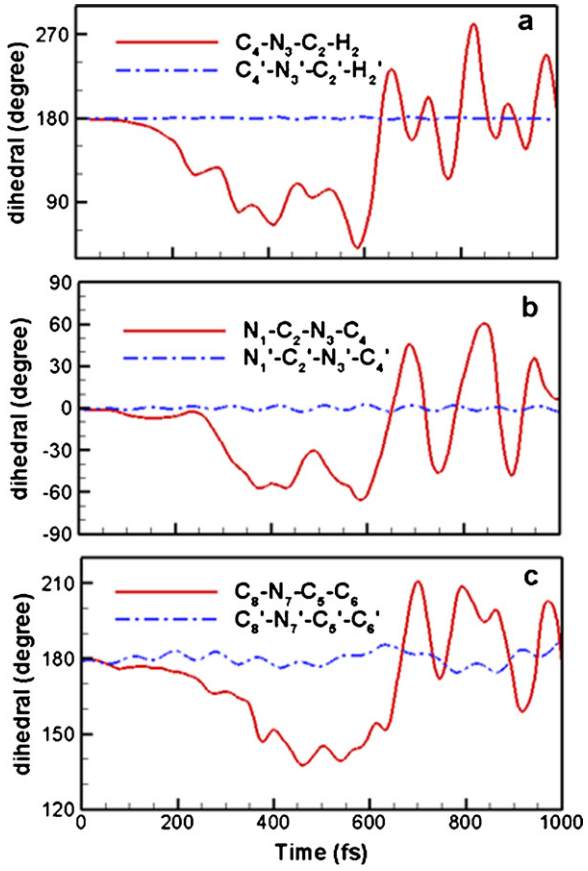

Fig. 4. Variation with time of the (a) C_4—N_3—C_2—H_2 and C_4'—N_3'—C_2'—H_2', (b) N_1—C_2—N_3—C_4 and N_1'—C_2'—N_3'—C_4', and (c) C_8—N_7—C_5—C_6 and C_8'—N_7'—C_5'—C_6' dihedral angles of the stacked adenines following application of a 25 fs (fwhm) laser pulse with a fluence of 31.68 J/m^2 and photon energy of 3.9 eV.

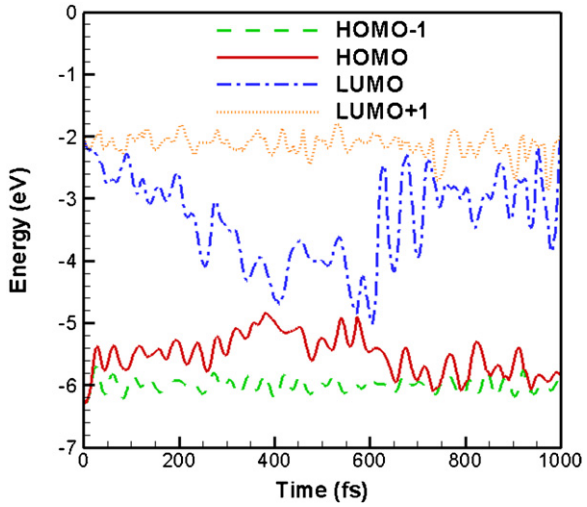

Fig. 5. The variations with time of the orbital energy of the HOMO−1, HOMO, LUMO and LUMO+1 of two stacked adenine molecules, one of which is subjected to a 25 fs (fwhm) laser pulse with a fluence of 31.68 J/m^2 and photon energy of 3.9 eV.

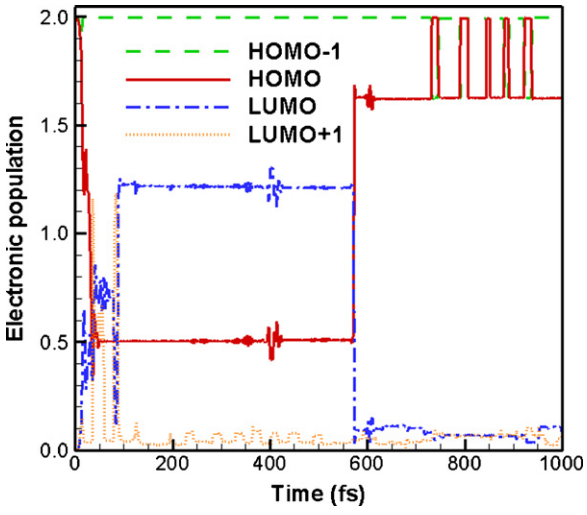

Fig. 6. The variations with time of the electronic populations of the HOMO−1, HOMO, LUMO and LUMO+1 of two stacked adenine molecules, one of which is subjected to a 25 fs (fwhm) laser pulse with a fluence of 31.68 J/m^2 and photon energy of 3.9 eV.

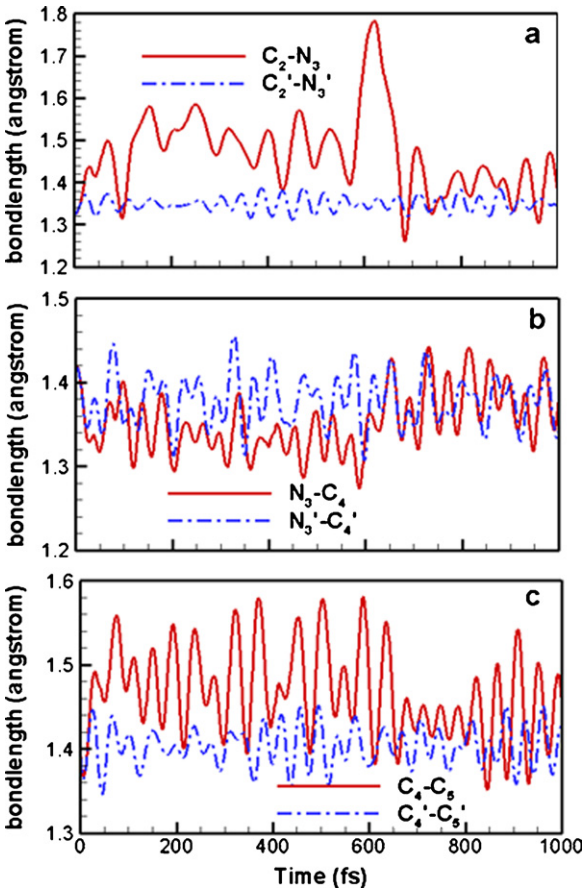

Fig. 7. Variation with time of the (a) C_2—N_3 and C_2'—N_3', (b) N_3—C_4 and N_3'—C_4' and (c) C_4—C_5 and C_4'—C_5' bond lengths of the stacked adenines following application of a 25 fs (fwhm) laser pulse with a fluence of 31.68 J/m2 and photon energy of 3.9 eV.

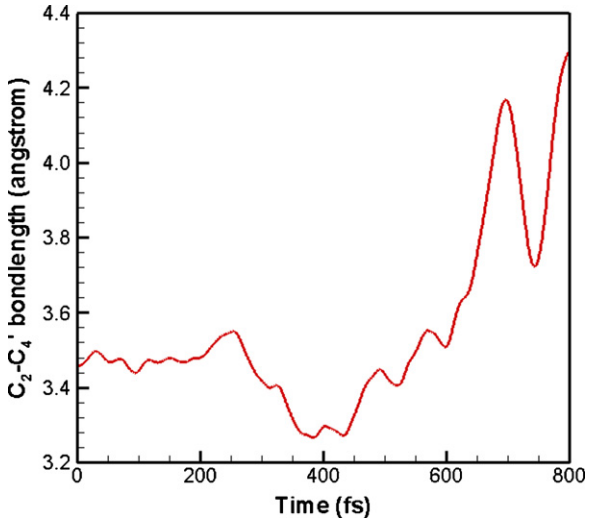

Fig. 8. Variation with time of the C_2—C_4' distance following the application of a 25 fs (fwhm) laser pulse with a fluence of 31.68 J/m^2 and photon energy of 3.9 eV.

longer has a planar structure (Fig. 4). The excited molecule evolves along the $\pi\pi^*$ state toward the conical intersection connecting to the ground state. This pathway is not limited to a single coordinate; it involves concurrent changes in at least three vibrational modes, viz., the out-of-plane vibration of the H_2 atom, the deformation vibration of the pyrimidine ring at the C_2 site, and the torsional vibration around the C_5—N_7 bond. The excited molecule decays to the electronic ground state through an avoided crossing in the vicinity of the conical intersection. This is induced by the coupling between the LUMO and HOMO (at ~580 fs) due to the out-of-plane vibration of H_2 atom and the deformation of the pyrimidine ring at the C_2 site. The other trajectories show a similar decay process at very slightly different time scales. There is no significant interaction between the excited and unexcited adenines during the excitation and de-excitation process. This is manifested by the lack of significant changes in the C_4'—N_3'—C_2'—H' and C_2'—N_3'—C_4'—C_5' dihedral angles, the HOMO and LUMO energy levels, and the C_2'—N_3', C_4'—C_5', and N_3'—C_4' bond lengths. The lack of the interaction between the excited and unexcited molecules is a result of the poor stacking of the two molecules because they move away from each other after the laser excitation, as shown by the variations of the distance between the C_2 and C_4' atoms in Fig. 8.

3.2. Slow nonradiative deactivation involving covalent bonding

The analysis of a representative trajectory is summarized in Fig. 9 through 14. Six snapshots from the simulation are shown in Fig. 9. Starting from the geometry adapted from ground state B-form DNA (Fig. 9a), the top molecule is electronically excited by the laser pulse (fluence = 25.83 J/m^2). The excited molecule undergoes an out-of-plane vibration of the H_2 atom and a deformation of the pyrimidine ring at the C_2 site from 410 fs to 1000 fs (Fig. 9b and c), while the unexcited molecule remains relatively unchanged for this period of time. At 1420 fs, a bond has been formed between the C_2 and C_4' atoms and the planar structure of the unexcited adenine shows significant deformation at the C_4' atom (Fig. 9d). At 2320 fs, the two adenine molecules are almost perpendicular to each other and the H_2 atom vibrates perpendicular to the pyrimidine ring of the excited molecule (Fig. 9e). At 3530 fs, the bond between the C_2 and C_4' atoms has been broken and the two molecules move away from each other (Fig. 9f).

Fig. 10a–c shows the changes in the C_4—N_3—C_2—H_2, N_1—C_2—N_3—C_4, and C_8—N_7—C_5—C_6 dihedral angle with time respectively. It is seen from Figs. 9 and 10a that the H_2 atom vibrates about the pyrimidine ring soon after the laser excitation. At 800 fs, it starts to move out of the pyrimidine ring and reaches the maximum displacement from the pyrimidine ring at ~2500 fs. After 2500 fs, it returns to the pyrimidine ring and oscillates about the pyrimidine ring. Fig. 10b shows that the N_1—C_2—N_3—C_4 dihedral angle, initially at 0°, changes by about 30° soon after the laser excitation. It stays near this value until 1500 fs and then goes back to its initial value and twists in the opposite direction reaching ~60° at 2400 fs, then gradually returns to its initial value. The C_8—N_7—C_5—C_6 angle changes from 180° to 150° during the first 500 fs, goes back to and stays near 180° at ~1000 fs until 200 fs, then rises to about 210° at 2700 fs, and returns close to 180° at 3000 fs.

The variations with time of the HOMO−1, HOMO, LUMO, and LUMO+1 levels of the dimer are presented in Fig. 11a; populations of these frontier molecular orbitals are plotted in Fig. 11b. The gap between the HOMO and LUMO becomes less than 0.5 eV from 1500 fs to 2500 fs. The HOMO and LUMO move back to about their initial values after 3200 fs. It is seen from Fig. 10b that the laser excitation promotes about 1.5 electrons from the HOMO mostly to the LUMO and the coupling between the HOMO and LUMO at ~2400 fs leads to a transfer of electrons from the LUMO to the HOMO.

Fig. 12 shows the variation with time of the C_2—N_3 and N_3—C_4 bond lengths and Fig. 13 shows the time dependence of the C_4—C_5 and C_4—N_9 bonds of the excited molecule. The variations of corresponding bonds in the unexcited molecule are also shown. The C_2—N_3 bond stretches from an initial value of 1.33 Å to about 1.47 Å after 100 fs. It remains at this length until ~3100 fs, then returns to

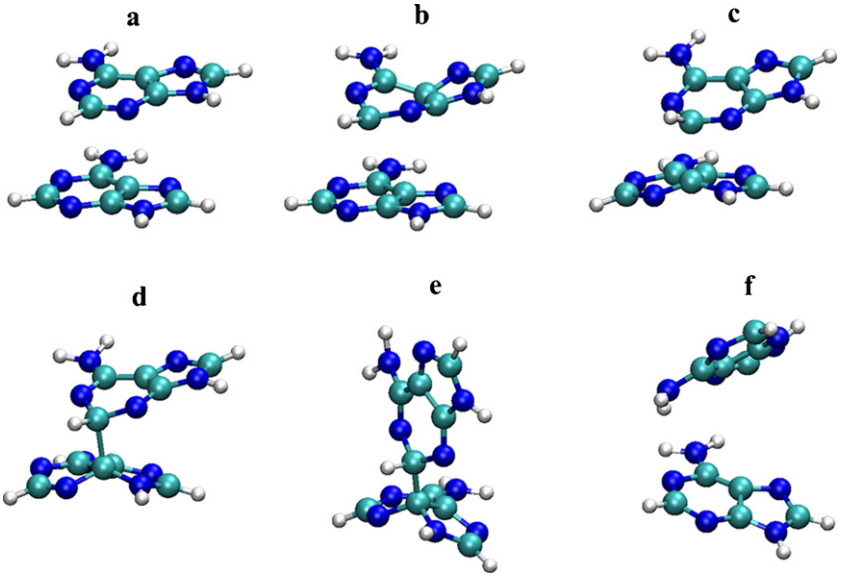

Fig. 9. Snapshots taken from the simulation of two stacked adenine molecules at (a) 0, (b) 480, (c) 1000, (d) 1420, (e) 2320, and (f) 3120 fs. The molecule at the bottom is subjected to the irradiation of a 25 fs (fwhm) laser pulse with a fluence of 25.83 J/m^2 and photon energy of 3.9 eV.

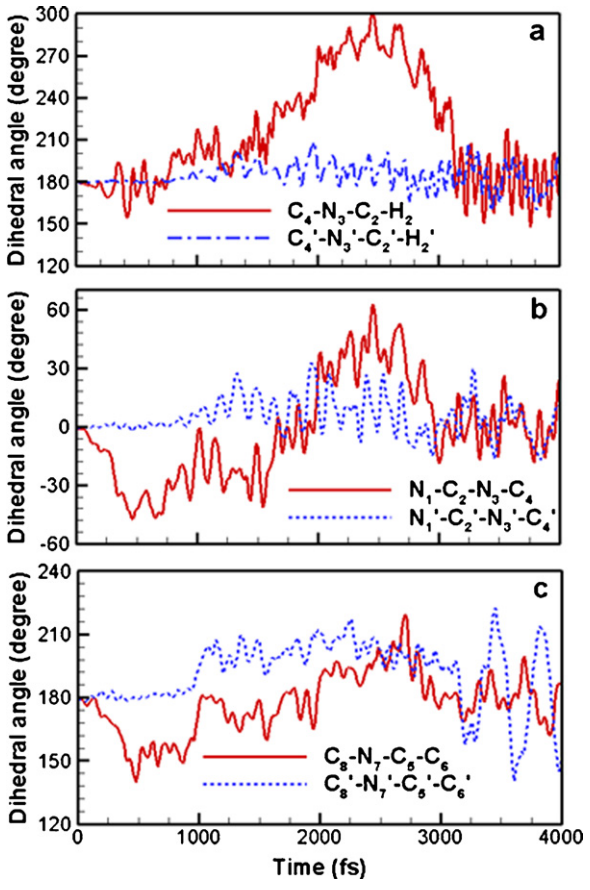

Fig. 10. Variation with time of the (a) C_4—N_3—C_2—H_2 and C'_4—N'_3—C'_2—H'_2, (b) N_1—C_2—N_3—C_4 and N'_1—C'_2—N'_3—C'_4 and (c) C_8—N_7—C_5—C_6 and C'_8—N'_7—C'_5—C'_6 dihedral angles of the stacked adenines following application of a 25 fs (fwhm) laser pulse with a fluence of 25.83 J/m^2 and photon energy of 3.9 eV.

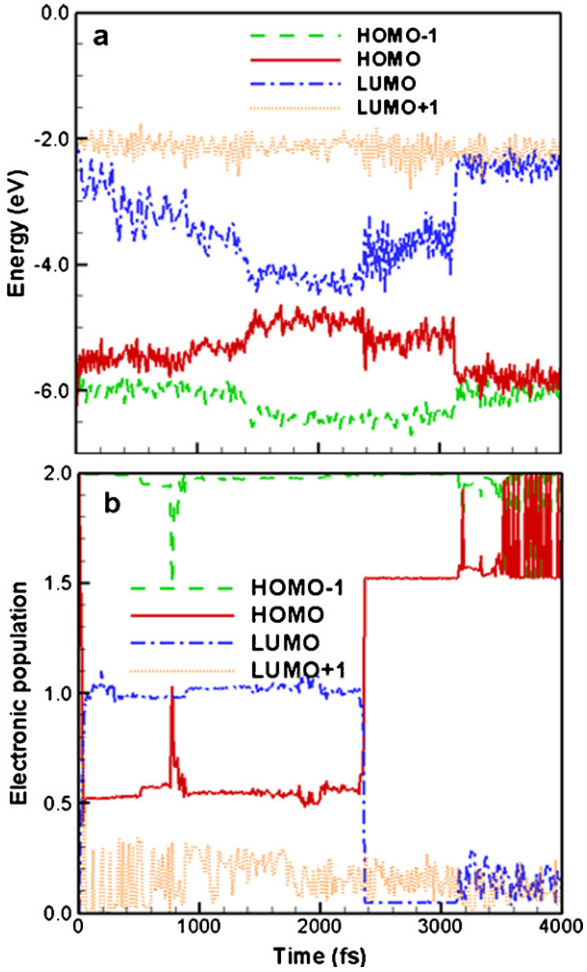

Fig. 11. The variations with time of (a) the orbital energy of the HOMO−1, HOMO, LUMO and LUMO+1 and (b) the electronic populations of two stacked adenine molecules, one of which is subjected to a 25 fs (fwhm) laser pulse with a fluence of 25.83 J/m^2 and photon energy of 3.9 eV.

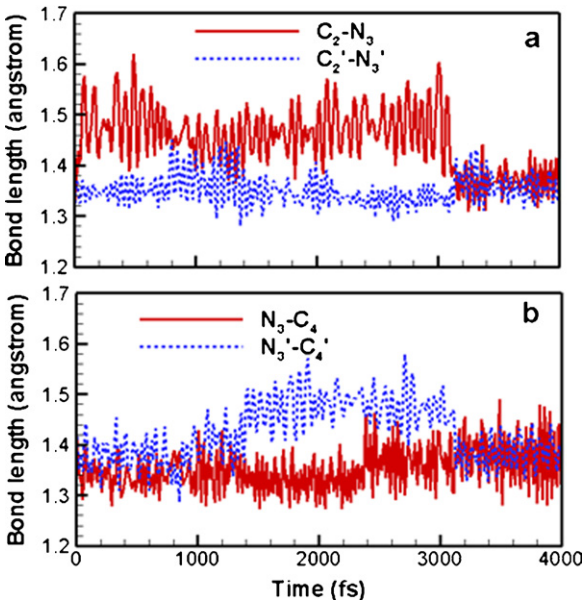

Fig. 12. Variation with time of the (a) C_2—N_3 and C_2'—N_3' and (b) N_3—C_4 and N_3'—C_4' bond lengths of the stacked adenines following application of a 25 fs (fwhm) laser pulse with a fluence of 25.83 J/m^2 and photon energy of 3.9 eV.

about its initial length. On the other hand, the same bond for the unexcited molecule only vibrates about its initial length for the entire simulation time. The C_4—C_5 bond lengthens from ~1.37 Å to ~1.47 Å soon after the laser excitation, becomes shorter after ~1000 fs, and finally goes back to its initial length from ~2500 fs. The C_4'—C_5' bond length increases from ~1.37 Å to ~1.48 Å after 1000 fs and decreases to its initial value after 3200 fs. The N_3—C_4 bond shrinks from 1.42 Å to 1.33 Å after 100 fs and stretches to about 1.40 Å after ~2400 fs The N_3'—C_4' bond stretches to ~1.47 Å from ~1000 fs to ~3200 fs. It is seen from Fig. 13b that the C_4—N_9 bond only vibrates about its initial length during the entire simulation run but the C_4'—N_9' bond has a significant lengthening from ~1000 fs to 3200 fs. The change in the N_3—C_4 bond length after

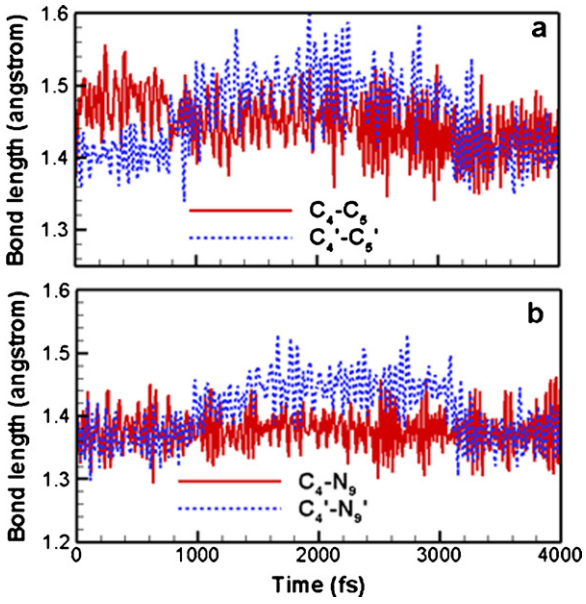

Fig. 13. Variation with time of the (a) C_4—C_5 and C_4'—C_5' and (b) C_4—N_9 and C_4'—N_9' bond lengths of the stacked adenines following application of a 25 fs (fwhm) laser pulse with a fluence of 25.83 J/m^2 and photon energy of 3.9 eV.

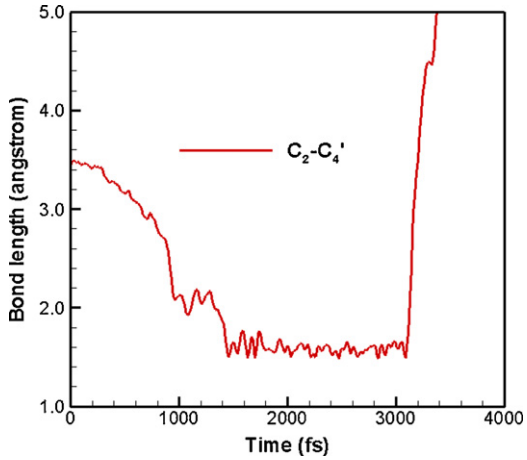

Fig. 14. Variation with time of the C_2—C_4' bond length of the stacked adenines following application of a 25 fs (fwhm) laser pulse with a fluence of 25.83 J/m^2 and photon energy of 3.9 eV.

2400 fs is a result of electron transfer from the LUMO to HOMO at 2400 fs.

The changes in the N_3'—C_4', C_4'—C_5', and C_4'—N_9' bond lengths after 1000 fs can be attributed to the formation of the excimer between two adenine molecules. Fig. 14 shows distance variations with time between the C_2 and C_4' atoms. The two adenine molecules move toward each other after laser excitation. A chemical bond with a length of ~1.5 Å is formed from ~1400 fs and remains until 3200 fs. After 3200 fs, the bond breaks and two molecules move away from each other rapidly. The formation of the C_2—C_4' bond between two adenines makes the N_3'—C_4', C_4'—C_5' and C_4'—N_9' bond lengths longer because of the breakage of the π–π conjugation of the unexcited adenine. The C_2—C_4' bond formation also slightly alters the C_2—N_1 and C_2—N_3 bond lengths. The interaction between the C_2 and C_4' sites of two stacked molecules limits the deformation of the pyrimidine ring at the C_2 site of the excited molecule, although another deformation occurs after ~800 fs at the same site but toward a different direction, as seen in Fig. 10b, and hinders the out-of-plane vibrations of the H_2 atom because of the steric effect of four chemical bonds connecting to the C_2 atom. The out-of-plane vibration of the H_2 atom reaches a maximum at ~2400 fs when the pyrimidine ring of the excited molecule becomes perpendicular to the pyrimidine ring of the unexcited molecule. This tetrahedral bonding geometry at the C_2 atom allows the C_2—H_2 bond to be perpendicular to the pyrimidine ring of the excited molecule. It should be mentioned here that, in reality, two stacked adenine molecules are connected through phosphate and ribose ring and the changes in their distance to each other and relative orientation should be significantly restricted. This indicates that the geometry showed in Fig. 9e is very unlikely and the deactivation of the excited molecule to the ground state should occur at a longer time scale.

The variation with time of the net charge of the A molecule is presented in Fig. 15. It can be seen that, after excitation, the charge fluctuates between the two molecules. However, there is a considerable charge transfer from A to A' between 2400 fs to 3100 fs, when the chemical bond is broken. It has been found both theoreticall and experimentally that charge transfer can occur through weak interactions such as hydrogen bonding [48,49] and π—π stacking between DNA bases [50]. The simulation results presented here are consistent with charge transfer between two stacked bases through chemical bond.

The simulation results presented in this section suggest the photophysical processes described below. By raising about 1.5 electrons from the HOMO to higher level frontier molecular orbitals, the laser pulse promotes the top molecule from the electronic

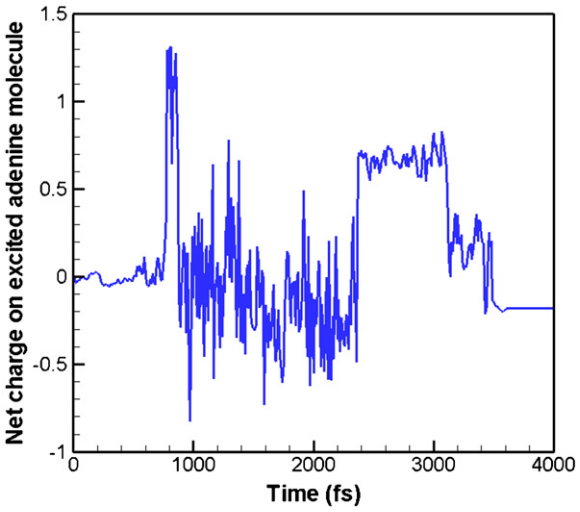

Fig. 15. The variation with time of the net charge of the excited adenine molecule.

ground state to a low-lying energy state $\pi\pi^*$. At this electronically excited state, the C_2—N_3 and C_4—C_5 bonds become longer, the C_2—N_3 bond becomes shorter and the pyrimidine and imidazole rings are no longer coplanar. The excited molecule moves along this reaction pathway, which is mainly controlled by the deformation of the pyrimidine ring at the C_2 site and the out-of-plane vibration of H_2 atom. The excited molecule starts to moves toward the unexcited molecule at about 800 fs; this is supported by the observations that the N'_3—C'_4, C'_4—C'_5 and C'_4—N'_9 bond lengths start to become longer and the unexcited molecule becomes nonplanar. At about 1500 fs, a covalent bond is formed between C_2 and C'_4 atoms, leading to the formation of the bonded excimer state. The formation of the covalent bond between two adenine molecules breaks the $\pi-\pi$ conjugation of the unexcited adenine and lengthens the N'_3—C'_4, C'_4—C'_5 and C'_4—N'_9 bonds. The energy gap between the LUMO and HOMO decreases significantly after 1500 fs, suggesting that the bonded excimer state is substantially lower than the excimer state in energy. After 1500 fs the system thus develops along the bonded excimer state toward the conical intersection to the electronic ground state. At about 2400 fs the system enters the vicinity of the conical intersection and then decays to the ground state through a channel resulted from the coupling between the LUMO and HOMO. The coupling occurs primarily because of the deformation of the pyrimidine ring at the C_2 site and the out-of-plane vibration of H_2 atom. The return to the electronic ground state of the excited molecule is confirmed by the increase in the N_3—C_4 bond length and the decrease in C_4—C_5 bond length after 2400 fs. Two adenines are still connected by the covalent bond even in the ground state after 2400 fs. The connected molecule becomes two adenine monomers after 3200 fs. The covalent bonding interaction between two adenines lowers the excited state energy and consequently stabilizes the excimer state, as discussed above. In addition, the deformation of the pyrimidine ring at the C_2 site makes the out-of-plane vibration of the H_2 atom more difficult; this slows down the nonradiative decay process. Other trajectories in this group have similar features although the deactivation time varies from 2100 fs to 2700 fs.

4. Discussion

The simulation results presented for the excitation by the laser pulse with a fluence of 31.68 J/m^2 demonstrate that two stacked adenine molecules follow a monomer-like nonradiative deactivation process, which has been extensively discussed in several high-level quantum chemical calculations [51–55,9,56,57,10] for monomer bases. These studies establish that for low energy excitation, the most efficient deactivation proceeds through the conical intersection accessed by a large-amplitude out-of-plane vibration of the H_2 atom because this structural distortion leads to the formation of an unstable biradical state. Based on their coupled-cluster calculations for CIS-optimized potential energy, Zgierski et al. [51] proposed that the biradical state has one unpaired electron occupying a π^* orbital localized on the imidazole ring and the second unpaired electron is mainly confined to a p-type atomic orbital on the C_2 atom of the pyrimidine ring. Their calculations further confirm [51] that at the minimum of the biradical state, the pyrimidine ring is strongly puckered and the C_2-H bond is twisted nearly perpendicular to the molecular plane. The present simulation study shows that at the vicinity of a conical intersection between the first electronic excited state and the ground state, where the molecule decays to the ground state because of the transfer of electrons from the LUMO to HOMO, the molecule has a very much similar geometry to one found by the quantum chemical calculations [51] indicating that, in this case, the decay follows a biradical pathway.

The simulation results presented for the excitation by the laser with a fluence of 25.83 J/m^2 show a slow decay process caused by stacking interaction, which results in the formation of a covalent bond between two adenine molecules. The bond formation and breaking significantly affect the coupling leading to the decays of excited system to the ground state, indicating the involvement of the bonded excimer in the nonradiative decay process of stacked bases.

The formation of a bonded excimer has been suggested to play an important role in some electron transfer processes. For example, Wang et al. [58] recently have found that the rapid charge-transfer quenching of the singlet excited states between cyanoaromatic electron acceptors and pyridine proceeds via the formation of bonded excimer. They explain that the formation of covalent bond between two species lowers the energy of the charge-transfer state significantly. They further argue that a bonded exciplex intermediate may be formed in a large number of other reactions that involve bond-making and bond-breaking processes. The observation of the formation of a covalent bond between two stacked adenines in our simulation supports the proposed involvement of bonded excimer formation in the nonradiative decay process of stacked bases.

The formation of the covalent bond between two stacked adenine molecules limits the conformational flexibility of each molecule. For example, it hinders the out-of-plane deformations of pyrimidine ring [25]. Comparing their QM/MM calculations for a single adenine residue in a $d(A)_{10}\cdot d(T)_{10}$ double strand and in isolated environment, Conti et al. [25] found that the L_a potential energy curve is flatter in DNA than in vacuo because of steric hindrance in the former. They argue that the small energy barrier of 0.2 eV in the L_a potential energy curve before the CI to the ground state is compatible with the slow decay channel observed in this system and therefore the slower decay channel is not necessarily accounted for only by excimer states. They suggested that the electrostatic interactions and steric hindrance limit the freedom of deformation needed to access the deactivating conical intersections to the ground state. The simulation results presented in this paper demonstrate both the formation of the bonded excimer and the steric effect affect the deactivation of stacked adenine molecules. It should be noted that, in reality, two stacked adenine molecules are connected through phosphate and ribose ring, which would significantly restrict changes in their distance and relative orientation. The large C_4—C_2—N_1—N_3 angle observed at about 2320 fs (corresponding geometry is showed in Fig. 2e) is very unlikely to occur and the deactivation of the excited molecule to the ground state should occur at a larger time scale.

The formation of the chemical bond between two moieties stabilizes the excimer state, which is evidenced by the decrease in the LUMO energy level, and has a positive contribution to long excited state lifetime. Based on their ab initio CASPT2 calculations, Olaso-González et al. [23] suggested that the excimer is a minimum in the potential energy surface cut on S_1 state; hence, a barrier can be expected in the decay path toward the CI. The energy barrier could be related to the long excited state lifetime observed experimentally.

In single-stranded polyadenine oligomers [$(dA)_n$], the formation of a chemical bond between two bases restricts the interaction of each of the bonded bases with un-bonded bases. This might favor the proposal [14] that the long-lived state in polyadenine oligomersare is localized on only two stacked bases. The formation of bonded excimer might lead to the dimerization of two adjacent bases, which is considered as the main cause of cell death, mutagenesis, and development of skin cancers [59]. The dimerization has been observed in stocked cytosines and thymines experimentally [60,61] and also shown by semiclassical dynamics simulations [62,63]. The bonded excimer state shown in the simulation study of two stacked adenine molecules of single-stranded polyadenine oligomers [$(dA)_n$], for which no experimental evidence for dimerization has yet been observed might have an important implication for photodamage.

5. Conclusion

The present investigation studies the effect of π-stacking on the nonradiative decay of adenine dimers and does not consider electrostatic interaction of adenine with the bonded sugar-phosphate groups and with the environment. Experimental observations show that the dynamics of a short-lifetime excited state of DNA bases is an intrinsic property of bases and is affected by interbase interaction, including base stacking and base pairing [14]. This property is not affected by other components of DNA. Experimental evidence also indicates that the base stacking is more important than the base pairing, where hydrogen bonds connect the bases of different strands [20]. Thus the present model works reasonably well for investigating the interaction between two stacked adenines. Our simulation focuses on the excitation of one of two π-stacked adenine molecules by one ultrafast laser pulse using two different laser fluences. In one case, the laser excitation leads to a poor interaction between the stacked molecules and the excited molecule shows a monomer-like nonradiative decay to the electronic ground state. In other case, the laser pulse leads to the formation of a covalent bond between the stacked molecules, indicating the involvement of a bonded excimer in the nonradiative decay. The simulations for these two cases start with the similar initial geometries of two stacked adenines; the different deactivation mechanisms are attributed to the different laser fluences. The fluence affects the population of the frontier molecular orbitals that results in different forces driving molecular motion. Thus, different fluences produce different stacking geometries, which lead to the different deactivation mechanisms. The simulation results show that stacking may result in steric hindrance to deformation which leads to nonradiative decay to the ground state. This suggests that both the bonded excimer state between two stacked adenine molecules and steric effect due to stacking influence the nonradiative decay of excited stacked-adenines.

Acknowledgements

This work was supported by the National Natural Science Foundation of China (Nos. 21073242 and 20773168). The Computer Facility at Chongqing University of Posts and Telecommunications provided computational assistance.

References

[1] R. Beukers, A.P.M. Eker, P.H.M. Lohman, DNA Repair 7 (2008) 530–543.
[2] C.E. Crespo-Hernández, B. Cohen, P.M. Hare, B. Kohler, Chemical Reviews 104 (2004) 1977–2019.
[3] R.J.H. Davies, J.F. Malone, Y. Gan, C.J. Cardin, M.P.H. Lee, S. Neidle, Nucleic Acids Research 35 (2007) 1048–1053.
[4] J.M. Pecourt, J. Peon, B. Kohler, Journal of the American Chemical Society 122 (2002) 9348–9349.
[5] Y. Lei, S. Yuan, Y. Dou, Y. Wang, Z. Wen, Journal of Physical Chemistry A 112 (2008) 8497–8504.
[6] H.R. Hudock, B.G. Levine, A.L. Thompson, H. Satzger, D. Townsend, N. Gador, S. Ullrich, A. Stolow, T.J. Martinez, Journal of Physical Chemistry A 111 (2007) 8500–8508.
[7] N. Ismail, L. Blancafort, M. Olivucci, B. Kohler, M.A. Robb, Journal of the American Chemical Society 124 (2002) 6818–6819.
[8] S. Perun, A.L. Sobolewski, W. Domcke, Chemical Physics 313 (2005) 107.
[9] S. Perun, A.L. Sobolewski, W. Domcke, Journal of the American Chemical Society 127 (2005) 6257.
[10] L. Serrano-Andrés, M. Merchán, A.C. Borin, Proceedings of the National Academy of Sciences of the United States of America 103 (2006) 8691–8696.
[11] L. Blancafort, B. Cohen, P.M. Hare, B. Kohler, M.A. Robb, Journal of Physical Chemistry A 109 (2005) 4431–4436.
[12] S. Ullrich, T. Schultz, M.Z. Zgierski, A. Stolow, Journal of the American Chemical Society 126 (2004) 2262–2263.
[13] N.K. Schwalb, F. Temps, Science 322 (2008) 243–245.
[14] C.T. Middleton, K. de La Harpe, C. Su, Y.K. Law, C.E. Crespo-Hernández, B. Kohler, Annual Review of Physical Chemistry 60 (2009) 217–239.
[15] I. Buchvarov, Q. Wang, M. Raytchev, A. Trifonov, T. Fiebig, Proceedings of the National Academy of Sciences of the United States of America 104 (2007) 4794–4797.
[16] S. Tonzani, G.C. Schatz, Journal of the American Chemical Society 130 (2008) 7607–7612.
[17] C.E. Crespo-Hernández, B. Kohler, Journal of Physical Chemistry B 108 (2004) 11182–11188.
[18] W.-M. Kwok, C. Ma, D.L. Phillips, Journal of the American Chemical Society 128 (2006) 11894–11905.
[19] F. Santoro, V. Barone, R. Improta, Proceedings of the National Academy of Sciences of the United States of America 104 (2007) 9931–9936.
[20] C.E. Crespo-Hernández, B. Kohen, B. Kohler, Nature 436 (2005) 1141–1144.
[21] B. Bouvier, J.P. Dognon, R. Lavery, D. Markovitsi, P. Millie, D. Onidas, K. Zakrzewska, Journal of Physical Chemistry B 107 (2003) 13512–13522.
[22] I. Buchvarov, Q. Wang, M. Raytchev, A. Trifonov, T. Fiebig, Proceedings of the National Academy of Sciences 104 (2007) 4794–4797.
[23] G. Olaso-González, M. Merchán, L. Serrano-Andrés, Journal of the American Chemical Society 131 (2009) 4368–4377.
[24] T. Takaya, C. Su, K. De La Harpe, C.E. Crespo-Hernández, B. Kohler, Proceedings of the National Academy of Sciences of the United States of America 105 (2008) 10285–10290.
[25] I. Conti, P. Altoè, M. Stenta, M. Garavelli, G. Orlandi, Physical Chemistry Chemical Physics 12 (2010) 5016–5023.
[26] Y. Dou, B.R. Torralva, R.E. Allen, Journal of Modern Optics 50 (2003) 2615.
[27] Y. Dou, B.R. Torralva, R.E. Allen, Chemical Physics Letters 392 (2004) 352.
[28] M. Graf, P. Vogl, Physical Review B 51 (1995) 4940–4949 (see also T.B. Boykin, R.C. Bowen, G. Klimeck, Phys. Rev. B 63 245314 (2001)).
[29] D. Porezag, Th. Frauenheim, Th. Kohler, G. Seifert, R. Kaschner, Physical Review B 51 (1995) 12947.
[30] M. Elstner, D. Porezag, G. Jungnickel, J. Elsner, M. Haugk, Th. Frauenheim, S. Suhai, G. Seifert, Physical Review B 58 (1998) 7260–7268.
[31] M. Haugk, J. Elsner, Th. Frauenheim, G. Seifert, M. Sternberg, Physical Status Solidi B 217 (1) (2000) 473–511.
[32] Th. Frauenheim, G. Seifert, M. Elstner, T.A. Niehaus, Ch. Köhler, M. Amkreutz, M. Sternberg, Z. Hajnal, A. Di Carlo, S. Suhai, Journal of Physics: Condensed Matter 4 (2002) 3015–3047.
[33] M. Wanko, M. Garavelli, F. Bernardi, T.A. Niehaus, Th. Frauenheim, M. Elstner, Journal of Chemical Physics 120 (2004) 1674–1692.
[34] G. Zheng, M. Lundberg, J. Jakowski, T. Vreven, M.J. Frisch, K. Morokuma, International Journal of Quantum Chemistry 109 (2009) 1841–1854.
[35] S. Yuan, Y. Dou, J. Zhao, Chinese Chemical Letters 19 (2008) 1379–1382.
[36] S. Yuan, Y. Dou, W. Wu, Y. Hu, J. Zhao, Journal of Physical Chemistry A 112 (2008) 13326–13334.
[37] Y. Dou, S. Xiong, W. Wu, S. Yuan, H. Tang, Journal of Photochemistry and Photobiology B 101 (2010) 31–36.
[38] W. Zhang, S. Yuan, A. Li, Y. Dou, J. Zhao, W. Fang, Journal of Physical Chemistry C 114 (2010) 5594–5601.
[39] R.E. Allen, T. Dumitrica, B.R. Torralva, in: K.T. Tsen (Ed.), Ultrafast Physical Processes in Semiconductors, Academic Press, New York, 2001 (Chapter 7).
[40] M. Born, J.R. Oppenheimer, Annalen der Physik (Leipzig) 84 (1927) 457–484.
[41] M. Born, K. Huang, The Dynamical Theory of Crystal Lattices, Oxford University Press, London, 1954.
[42] E. Teller, Journal of Physical Chemistry 41 (1937) 109–116.

[43] Conical intersections: electronic structure, dynamics & spectroscopy, in: W. Domcke, D.R. Yarkony, H. Köppel (Eds.), Advanced Series in Physical Chemistry, World Scientific, Singapore, 2004.
[44] M. Baer, Beyond Born-Oppenheimer: Electronic Nonadiabatic Coupling Terms and Conical Intersections, Wiley Interscience, Hoboken, 2006.
[45] M.J. Bearpark, F. Bernardi, S. Clifford, M. Olivucci, M.A. Robb, T. Vreven, Journal of Physical Chemistry A 101 (1997) 3841–3847.
[46] B.G. Levine, T.J. Martinez, Annual Review of Physical Chemistry 58 (2007) 613.
[47] M. Elstner, P. Hobza, T. Frauenheim, S. Suhai, E. Kaxiras, Journal of Chemical Physics 114 (2001) 5149.
[48] Z. Guang-Jiu, H. Ke-Li, Accounts of Chemical Research 45 (2012) 404.
[49] Z. Guang-Jiu, L. Jian-Yong, Z. Li-Chuan, H. Ke-Li, Journal of Physical Chemistry B 111 (2007) 8940–8945.
[50] R.E. Holmlin, P.J. Dandliker, J.K. Barton, Chemie International Edition England 36 (1997) 2714–2730.
[51] M.Z. Zgierski, S. Patchkovskii, E.C. Lim, Canadian Journal of Chemistry 85 (2007) 124.
[52] Z. Wenying, Y. Shuai, W. Zhijin, Q. Zhiming, Z. Jianshe, D. Yusheng, V.L. Glenn, Chemical Physics Letters 506 (2011) 303–308.
[53] K.A. Seefeld, C. Plützer, D. Löwenich, T. Häber, R. Linder, K. Kleinermanns, J. Tatchen, C.M. Marian, Physical Chemistry Chemical Physics 7 (2005) 3021–3026.
[54] M.P. Fülscher, L. Serrano-Andres, B.O. Roos, Journal of the American Chemical Society 119 (1997) 6168–6176.
[55] B. Mennucci, A. Toniolo, J. Tomasi, The Journal of Physical Chemistry A 105 (2001) 4749–4757.
[56] H. Chen, S. Li, Journal of Physical Chemistry A 109 (2005) 8443–8446.
[57] L. Blancafort, Journal of the American Chemical Society 128 (2006) 210–219.
[58] Y. Wang, O. Haze, J.P. Dinnocenzo, S. Farid, Journal of Organic Chemistry 72 (2007) 6970–6981.
[59] V.O. Melnikova, H.N. Ananthaswamy, Mutation Research 571 (2005) 91–106.
[60] J.-L. Ravanat, T. Douki, Journal of Photochemistry and Photobiology B: Biology 63 (2001) 88–102.
[61] D.H. Lee, G.P. Pfeifer, The Journal of Biological Chemistry 278 (2003) 10314–10321.
[62] Z. Wenying, Y. Shuai, L. Anyang, D. Yusheng, Z. Jianshe, F. Weihai, Journal of Physical Chemistry C 114 (2009) 5594–5601.
[63] Y. Shuai, Z. Wenying, L. Lihong, D. Yusheng, F. Weihai, V.L. Glenn, Journal of Physical Chemistry A 115 (46) (2011) 13291–13297.